20th Australasian Fluid Mechanics Conference
Perth, Australia
5-8 December 2016

Proper Orthogonal Decomposition Analysis of Sound Generation in a Turbulent Premixed Flame

D. Brouzet[1], A. Haghiri[1], T. Colonius[2], M. Talei[1] and M. J. Brear[1]

[1]Department of Mechanical Engineering
University of Melbourne, Victoria 3010, Australia

[2]Division of Engineering and Applied Science
California Institute of Technology, Pasadena, CA 91125, USA

Abstract

This paper presents proper orthogonal decomposition (POD) method of a Direct Numerical Simulation (DNS) dataset of a turbulent premixed flame. The POD results show that the combustion process is the dominant source of noise at low frequencies, whereas the inlet noise becomes an increasingly important source at higher frequencies. It is also shown that the first three POD modes, that are mainly associated with the noise produced by the flame, can provide a reasonable estimate of the DNS spectra at low frequencies.

Introduction

Lean premixed combustion is a promising way of decreasing regulated pollutant emission in modern gas turbines. However, combustors operating with lean flames are susceptible to thermo-acoustic instabilities [8]. This phenomenon involves a strong coupling between the flame dynamics and acoustic waves and results in large pressure fluctuations leading to the combustor failure in extreme cases [7, 10]. As a result, achieving a better understanding of how flames produce sound is of great importance for environmental and safety reasons.

A number of different frameworks have been used to analyse combustion-generated noise. One of these involves employing a form of acoustic analogy, obtained by rearranging the equations of motion into different forms of the inhomogeneous wave equation. The source terms in an acoustic analogy may be then interpreted as the main sources of sound in a given flow. For instance, in an early work by Strahle [9], the fluctuations of the heat release rate was identified as the dominate source of noise in combustion by using Lighthill's acoustic analogy [6]. Much of the subsequent works started from that basis and provided useful insight [11].

Proper orthogonal decomposition (POD) is a widely known tool that decomposes a dataset into a series of independent, orthogonal modes. In many mechanical systems, this technique is used to identify the most energetic behaviours of physical variables of a system. POD is also a potential tool to analyse sound generated by flames as it can show how different flow events that occur with regular frequency and are mutually correlated over large spatial extent contribute to the generated sound. While acoustic analogies provide some information about the distribution of sound sources in a flow, POD can provide more details about the contribution of coherent structures to the produced sound. For example, Kabiraj et al. performed a POD analysis on flame images in an experimental study of a turbulent premixed flame [3]. They further established a link between the coherent structures observed in the flame and pressure fluctuations at a given location in the far field. However, the POD analysis in their study as well as others reported in the literature, in the context of turbulent combustion, have been limited to the flame region.

This paper therefore applies POD to the pressure fluctuations over the entire computational domain of a DNS dataset that captures a turbulent, premixed flame producing sound [2]. This enables unambiguous determination of any correlation between the far-field sound and structures in the flame.

Numerical methods

DNS dataset

A DNS dataset of a turbulent premixed stoichiometric flame featuring sound generation was used in this study [2]. The DNS was performed using a modified version of S3D [1], referred to as S3D-SC [4]. It uses an 8^{th} order central differencing scheme for spatial derivatives, combined with a 6-stage, 4^{th} order explicit Runge-Kutta time integrator.

Jet diameter	D
Domain size $(L_x \times L_y \times L_z)$	$25D \times 16D \times 16D$
Grid resolution $(n_x \times n_y \times n_z)$	$2628 \times 1040 \times 1040$
Mean inlet Mach number (M)	0.35
Co-flow Mach number	0.0035
Heat release parameter (α)	2.08
Jet Reynolds number (Re)	5300
Inlet turbulent intensity $(u'/\overline{U}_j)$	3.7% (at centreline)
Thermal flame thickness (δ_{th}/D)	0.07
Sound speed (a_{ref})	1.755
Laminar flame speed (S_L/a_{ref})	0.00422
Zeldovich number (β)	7.9
Damkholer number (Da)	8.6
Prandtl number (Pr)	0.72
Lewis number (Le)	1

Table 1: DNS parameters.

The DNS data features a round jet of unburned premixed mixture (reactant) at stoichiometric condition issuing into an open environment of combustion products at the adiabatic flame temperature. The jet Reynolds number was equal to 5300 and a homogeneous turbulence field with a turbulence intensity of 3.7% at the jet centreline was fed into the mean velocity field using the Taylor hypothesis. Four jet flow-through times were used for post-processing. Table 1 summarizes the DNS parameters. A representation of the flame at the jet centreline with the isosurface of maximum reaction rate can be seen in figure 1.

POD formulation

To study the flame acoustics, the POD analysis was performed on the pressure fluctuations field p' of a 2D plane passing through the flame centreline. Both temporal and spectral

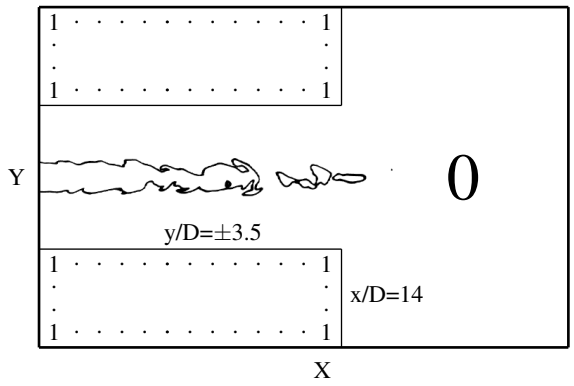

Figure 1: Weighting matrix used in the POD formulation.

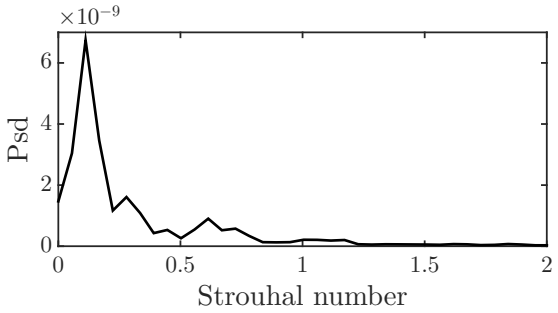

Figure 2: Pressure spectrum at location $[14D;6D]$.

POD approaches were used to analyse the data. In temporal POD, the data matrix $\mathbf{Q}$ used in the formulation is composed of spatial vectors of p' at different instants such that: $\mathbf{Q} = [\mathbf{P}'(t_1) \ \ldots \ \mathbf{P}'(t_N)]$. The vectors $\mathbf{P}'(t_i)$ represent the 2D p' field at instant t_i, i.e. $\mathbf{P}'(t_i) = [p'(x_1,y_1) \ldots p'(x_m,y_n)]^T_{t=t_i}$ where m and n are the number of grid points in the streamwise and spanwise directions, respectively.

In spectral POD, spectra of the pressure fluctuations $\mathcal{P}'$ are first computed at each point in space using a number of realizations N_f from the pressure field. They are then used to construct the data matrix $\mathbf{Q}$ for a particular frequency f_p, such that: $\mathbf{Q} = [\boldsymbol{P}'_1(f_p) \ldots \boldsymbol{P}'_{N_f}(f_p)]$. Vectors $\boldsymbol{P}'_i(f_p)$ represent the power spectral density value at frequency f_p for the i^{th} realization, i.e. $\boldsymbol{P}'_i(f_p) = \left[\mathcal{P}'(x_1,y_1,f_p) \ldots \mathcal{P}'(x_m,y_n,f_p)\right]^T_i$. In that case, the modes found are representative of the pressure field behaviour at a given frequency f_p.

In classical POD, the most energetic recurring behaviours of a system are found by solving the following eigenvalue problem [5]:

$$\mathbf{K\Psi} = \mathbf{Q}^T\mathbf{Q\Psi} = \mathbf{\Psi\lambda}. \tag{1}$$

In equation 1, $\mathbf{K}$ is the covariance matrix, $\mathbf{\Psi}$ is the eigenvectors' matrix and $\mathbf{\lambda}$ is the eigenvalues' diagonal matrix.

In this paper, a particular focus was on pressure fluctuations outside the flame. For this purpose, a weighting matrix $\mathbf{H}$ was defined as equal to 1 if $x/D < 14$ and $\mid y/D \mid > 3.5$, and equal to 0 otherwise (see figure 1). Then the diagonal weighting matrix $\mathbf{H_s}$ was constructed from $\mathbf{H}$ and the covariance matrix $\mathbf{K}$ was changed to:

$$\mathbf{K} = \mathbf{Q}^T\mathbf{H_sQ}. \tag{2}$$

This can be seen as a correlation between $\mathbf{H_sQ}$ and $\mathbf{Q}$, the first matrix being composed of p' values in the unity weighting region. In this way the POD analysis shows how the sound in the specific unity weighting region correlates with the pressure in the whole computational domain.

Then, the i^{th} proper orthogonal modes Φ_i was found by multiplying $\mathbf{Q}$ to the i^{th} eigenvector and normalizing it:

$$\Phi_i = \frac{\mathbf{Q}\Psi_i}{\parallel (\mathbf{Q}\Psi_i)^T\mathbf{H_sQ}\Psi_i \parallel^{1/2}}. \tag{3}$$

The relative importance of the i^{th} mode was given by the ratio of its corresponding eigenvalue λ_i by the sum of all eigenvalues.

Using both equations 1 and 3, it can be shown that:

$$\mathbf{\Phi}^T\mathbf{H_s\Phi} = \mathbf{I}. \tag{4}$$

With this weighted formulation, the modes are not orthogonal to each other in the entire domain, as in classical POD. This relation can be seen as the modes being independent to each other only outside the jet wake, where $H_{ij} = 1$ (see figure 1).

Finally, the POD coefficients $\mathbf{a} = [a_1 \ a_2 \ldots a_N]^T$, where vectors a_i represent the time coefficients for mode Φ_i, were computed. Taking the ansatz $\mathbf{Q} = \mathbf{\Phi a}$, it can be shown that the time coefficients a_i for the corresponding mode Φ_i is given by the following equation:

$$a_i = \Phi_i^T\mathbf{H_sQ}. \tag{5}$$

If equation 5 is used to rearrange the ansatz, the following relation is obtained:

$$\mathbf{\Phi a} = \mathbf{\Phi\Phi}^T\mathbf{H_sQ}. \tag{6}$$

So the ansatz and equation 5 will be valid if and only if $\mathbf{\Phi\Phi}^T\mathbf{H_s} = \mathbf{I}$, which will be the case in the unity weighting region.

A reconstruction matrix $\mathbf{Q_r}$ with M modes may be obtained using the following equation:

$$\mathbf{Q_r} = \sum_{i=1}^{M} \Phi_i a_i. \tag{7}$$

Note that summing over all modes would give a perfect reconstruction so that $\mathbf{Q_r} = \mathbf{Q}$ in the unity weighting region.

Results and discussion

A typical spectrum of the acoustic pressure fluctuations outside the flame, at location $[14D;6D]$, is shown in figure 2. This was computed by averaging Fast Fourier Transform (FFT) of 14 realizations including 512 timesteps each. A hanning window was used to avoid any spurious high frequency content and an overlap of 75 % between consecutive time intervals was used. With the choice of these parameters, both a good spectrum convergence and spectral resolution were achieved. The dimensionless Strouhal number used throughout this paper was defined based on the inlet diameter D and the Mach number M such that:

$$St = \frac{fD}{M} \tag{8}$$

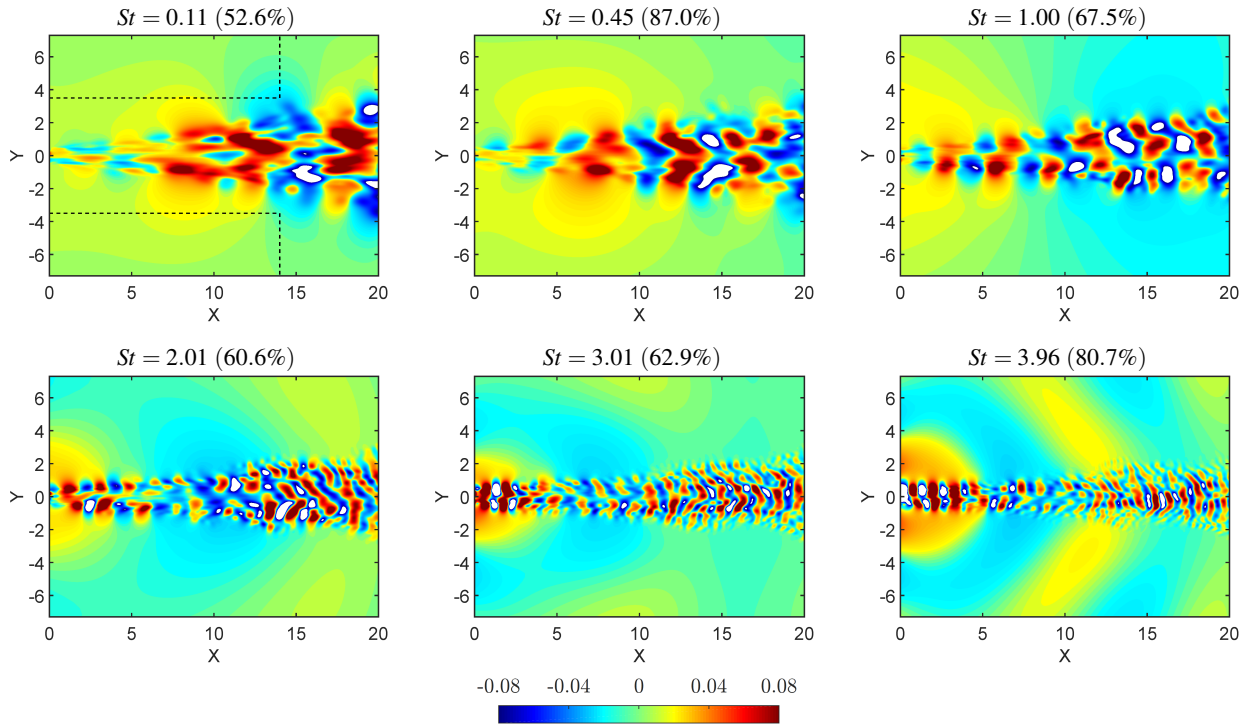

Figure 3: Most energetic spectral POD modes at various Strouhal numbers.

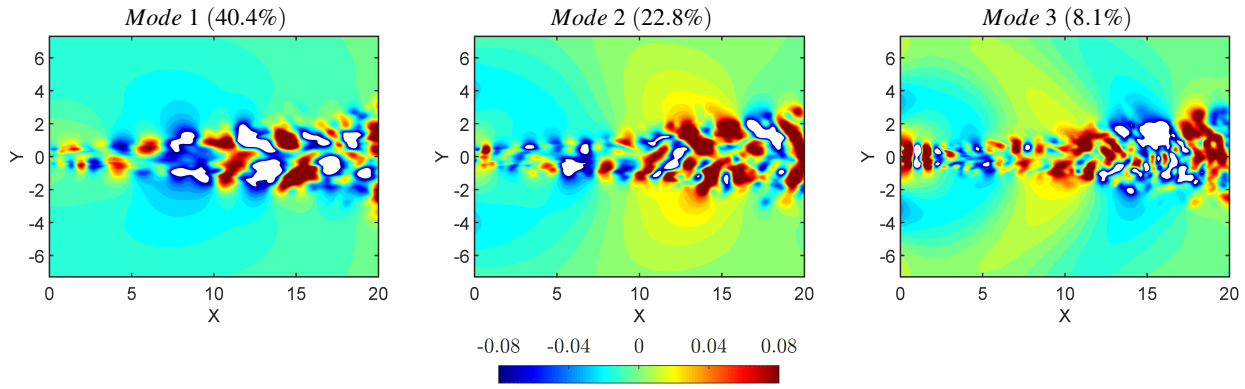

Figure 4: Three most energetic temporal POD modes.

The most energetic mode for Strouhal numbers equal to 0.11, 0.45, 1.00, 2.01, 3.01 and 3.96 can be seen in figure 3, showing flame acoustics behaviour for a wide range of frequencies. The relative importance of the first mode compared with the other modes at a given frequency is displayed as a percentage on top of each subplot. The weighting region is also shown on the top left subplot. The two modes corresponding to lower frequencies show pressure waves coming from the flame, indicating that the combustion process is mainly responsible for the sound produced at those frequencies. It can be especially noted that the most energetic mode at $St = 0.45$ is accountable for 87% of the produced noise at that frequency, illustrating how important the sound coming from the flame is at low frequencies. However, at $St = 1.00$ and $St = 2.01$, the inlet noise appears to increasingly contribute to the sound generation process. At $St = 2.01$, the inlet and the combustion noise seem to be of comparable strength (orange and blue areas respectively at inlet and flame tip). The inlet noise then becomes stronger at $St = 3.01$ and finally is the dominant source of noise at $St = 3.96$. Here, the fact that the most energetic mode at $St = 3.96$ is responsible for 80% of the produced sound shows that the inlet noise dominates the combustion-generated noise at high frequencies. Overall, figure 3 shows that the two phenomena responsible for the produced noise contribute differently relative to each other at different frequencies. However, the spectral POD does not shed light on the strength of these sources to the overall produced sound.

Temporal POD will provide an answer to this question by showing the most energetic modes, without breaking down the dominant structures based on their frequency. The results of temporal POD with the relative importance of each mode are displayed in figure 4. Mode 1 is accountable for 40.4% of the noise coming from the central region of the flame. The second mode is almost twice less important and displays sound generation from the tip and inlet. The third mode features a pure inlet noise behaviour but is only accountable for 8.1% of the overall sound, confirming that the inlet noise is far less

important than the combustion noise in the stoichiometric turbulent premixed flame studied here.

The combined contribution of the three most energetic modes is equal to 71.3%, suggesting that the reconstruction of the data with these three modes might give a reasonable estimation of the DNS data. The average spectrum of the reconstructed signal at the point $[14D;6D]$ was computed and is plotted in figure 5, with the DNS data spectrum shown as a reference. It can be seen that there is a good agreement between the reconstructed data and DNS for frequencies less that 0.7. However, the reconstructed signal is not representative for higher frequencies. This was expected, as the most energetic modes mainly represent the noise produced by the combustion process which was shown to be associated to lower frequencies (see figure 5).

The individual spectra of modes 1 to 3, displayed in figure 6, show different peak frequencies. The main peak at $St = 0.11$ is mainly represented by mode 1 while the second peak at $St = 0.61$ is almost due to mode 3.

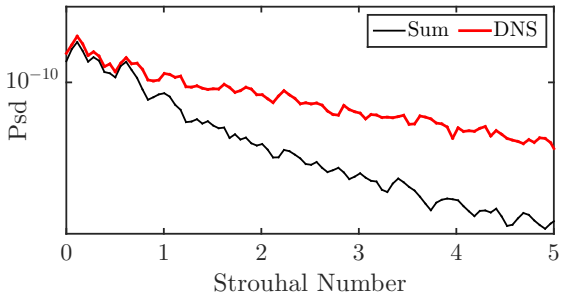

Figure 5: Time signal reconstruction with 3 most energetic modes of temporal POD compared with DNS data in the spectral domain.

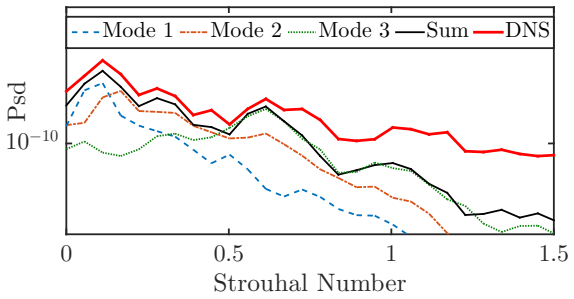

Figure 6: Individual mode spectra compared to time signal reconstruction and DNS spectra.

Conclusion

Spectral and temporal proper orthogonal decomposition (POD) was used to study noise production by a turbulent, premixed flame. These decompositions were performed on a recently developed DNS dataset that resolved both the turbulent flame motions and its radiated sound.

This analysis revealed that the dominant acoustic modes at low frequencies were mainly associated with combustion, whereas the inlet forcing played an important role at higher frequencies. Both sources were of comparable importance at intermediate frequencies. Reconstructed acoustic spectra from the 3 most energetic POD modes also gave reasonable agreement with the DNS data at low frequencies.

Further investigations will consider sound production by lean flames, which are important when considering real devices. They will also attempt to relate this POD approach to a more physical understanding of the relationships between the radiated sound and the flame structure.

Acknowledgements

The research was supported by computational resources on the Australian NCI National Facility through the National Computational Merit Allocation Scheme and Intersect Australia partner share and by resources at the Pawsey Supercomputing Centre.

References

[1] Chen, J. H., Choudhary, A., De Supinski, B., DeVries, M., Hawkes, E. R., Klasky, S., Liao, W.-K., Ma, K.-L., Mellor-Crummey, J., Podhorszki, N. et al., Terascale direct numerical simulations of turbulent combustion using s3d, *Computational Science & Discovery*, **2**, 2009, 015001.

[2] Haghiri, A., Talei, M., Brear, M. J. and Hawkes, E. R., Direct numerical simulation of noise generation by turbulent premixed flames, *To be submitted to Journal of Fluid Mechanics*.

[3] Kabiraj, L., Saurabh, A., Nawroth, H. and Paschereit, C. O., Recurrence analysis of combustion noise, *AIAA Journal*, **53**, 2015, 1199–1210.

[4] Karami, S., Talei, M., Hawkes, E. R. and Chatakonda, O., Direct numerical simulation of a partially premixed turbulent, lifted flame, in *Proceedings of the 9th Asia-Pacific Conference on Combustion, Gyeongju, South Korea*, 2013.

[5] Kerschen, G. and Golinval, J.-C., Physical interpretation of the proper orthogonal modes using the singular value decomposition, *Journal of Sound and Vibration*, **249**, 2002, 849–865.

[6] Lighthill, M. J., On sound generated aerodynamically. i. general theory, in *Proceedings of the Royal Society of London A: Mathematical, Physical and Engineering Sciences*, The Royal Society, 1952, volume 211, 564–587, 564–587.

[7] Nicoud, F. and Poinsot, T., Thermoacoustic instabilities: Should the rayleigh criterion be extended to include entropy changes?, *Combustion and Flame*, **142**, 2005, 153–159.

[8] Poinsot, T. and Veynante, D., *Theoretical and numerical combustion*, RT Edwards, Inc., 2005.

[9] Strahle, W. C., On combustion generated noise, *Journal of Fluid Mechanics*, **49**, 1971, 399–414.

[10] Swaminathan, N., Xu, G., Dowling, A. and Balachandran, R., Heat release rate correlation and combustion noise in premixed flames, *Journal of Fluid Mechanics*, **681**, 2011, 80–115.

[11] Talei, M., Brear, M. J. and Hawkes, E. R., Sound generation by laminar premixed flame annihilation, *Journal of Fluid Mechanics*, **679**, 2011, 194–218.